Structural and Microstructural Characterization of the Growth Lines and Prismatic Microarchitecture in Red Abalone Shell and the Microstructures of Abalone "Flat Pearls"

Xiaowei Su,[†,||] Angela M. Belcher,[‡,§,⊥] Charlotte M. Zaremba,[‡] Daniel E. Morse,[§] Galen D. Stucky,[‡] and Arthur H. Heuer*[,†]

Department of Materials Science and Engineering, Case Western Reserve University, Cleveland, Ohio 44106, and Department of Chemistry and Marine Biotechnology Center, University of California, Santa Barbara, Santa Barbara, California 93106

Received December 27, 2001. Revised Manuscript Received April 12, 2002

The structure of the growth lines in the shell of the red abalone, *Haliotis rufescens*, has been characterized by X-ray diffraction analysis and by scanning and transmission electron microscopy. The growth lines consist of a blocklike microstructure and a spherulitic microstructure, separated by a green organic matrix interlayer. The minerals in both the blocklike and spherulitic structures have been determined to be aragonite, the same $CaCO_3$ polymorph as in the nacreous microstructure in these shells. The spherulitic structure is composed of radially distributed elongated crystals, whereas the blocklike structure involves crystalline aggregates with irregular shape. The individual aggregates are approximately single crystal, with orientations identical to that of the adjacent stack of tablets in the nacreous structure. The interfaces defining the transition from nacreous to blocklike microstructures are abrupt; on the other hand, the transition from spherulitic to nacreous microstructures shows more irregularity because of the occasional intergrowth of elongated crystals into the nacreous region. The microstructures of "flat pearls", produced by mineralization of an abiotic substrate (a glass cover slip) inserted between the mantle tissue and the growing edge of the shell in a live abalone, have also been studied. A thin calcitic $CaCO_3$ layer is produced on the center of the glass substrate, which is soon covered by green organic matrix. This *matrix* extends beyond the calcitic region; that is, it can be secreted directly onto the glass. Mineralization of this green matrix layer involves the deposition of spherulitic aragonite, similar to that occurring in the native shell, which is then capped by nacreous aragonite. Thus, the microstructures within the flat pearls mimic very closely certain aspects of the microstructures within the growth lines of the native shell.

Introduction

Abalone is a gastropod mollusc whose shell is a biocomposite consisting of both organic macromolecules (proteins, glycoproteins, and polysaccharides) and $CaCO_3$.[1−3] (There are three polymorphs of $CaCO_3$—calcite, aragonite, and vaterite.) In detail, the abalone shell contains an outermost nonmineralized layer called the periostracum, which is adjacent to a calcitic prismatic layer that abuts the innermost aragonitic nacreous layer. The periostracum is an organic membrane, 0.1−0.2-μm thick, that protects the shell. The calcitic prismatic layer in red abalone shell contains a small quantity of organic components[3] and has not yet been studied in detail using high-resolution electron microscopy. The nacreous layer, on the other hand, consists of stacks of aragonite tablets, ≈0.4-μm thick and 5−10-μm wide, separated from their neighbors by thin organic membranes. Interspersed within the nacre are other features called growth lines,[4] which include blocklike and spherulitic morphologies, in marked contrast to the tabular morphology of the nacreous microstructure. (Growth lines are periodic growth structures produced by a living organism and are a record of cyclic changes that occur in growth rate and/or density and composition of the grown material.) Although the growth lines in abalone shell have been used by biologists to estimate the ages of individual organisms,[4−6] there have been few

* To whom correspondence should be addressed. E-mail address: heuer@cwru.edu.
† Case Western Reserve University.
‡ Department of Chemistry, University of California, Santa Barbara.
§ Marine Biotechnology Center, University of California, Santa Barbara.
|| Present address: The Lerner Research Institute, The Cleveland Clinic Foundation, 9500 Euclid Ave., Cleveland, OH 44115.
⊥ Present address: Department of Chemistry, The University of Texas at Austin, Austin, TX 78713-8926.

(1) Zaremba, C. M.; Belcher, A. M.; Fritz, M.; Li, Y.; Mann, S.; Hansma, P. K.; Morse, D. E.; Speck, J. S.; Stucky, G. D. *Chem. Mater.* **1996**, *8*, 679.
(2) Shepherd, S. A.; Avalos-Borja, M.; Quintanilla, M. O. *Mar. Freshwater Res.* **1995**, *46*, 607.
(3) Mutvei, H. *Origin, Evolution and Modern Aspects of Biomineralization in Plants and Animals*; Crick, R. E., Ed; Plenum Press: New York, 1989; pp 137−151.
(4) Erasmus, J.; Cook, P. A.; Seijd, N. *J. Shellfish Res.* **1994**, *13*, 493.
(5) Prince, J. D.; Sellers, T. L.; Ford, W. B.; Talbot, S. R. *Aust. J. Mar. Freshwater Res.* **1988**, *39*, 167.
(6) Shepherd, S. A.; Al-Wahibi, D.; Al-Azri, A. R. *J. Shellfish Res.* **1994**, *34*, 461.

10.1021/cm011739q CCC: $22.00
Published on Web 05/23/2002

comprehensive high-resolution studies of the microstructure of these features in native shells.

The most detailed studies relating to these growth lines in red abalone shell have entailed experiments involving deposition of shell biominerals on abiotic substrates (to form the so-called "flat pearls") inserted between the growing edge of the shell and the epithelial cells of the mantle, a thin secretory tissue lining the inner surface of the shell.[1,7] Both the organic material that was initially deposited at the center of the abiotic substrate and the inorganic phase that first formed on top of this organic phase differed considerably in texture and morphology from those components secreted onto the lateral margins of the implant. Thus, the edge of the "flat pearl" closest to the outside edge of the shell is red in color, with a blocklike calcitic structure; these features are similar to those observed for the exterior of the shell. Two types of organic sheets, *transparent* and *green colored*, are deposited on the region of the glass cover slip substrate apposed to nacre. The transparent sheet (≈140-nm thick) is deposited first, in a central 7−12-mm-diameter region of the substrate. Within 1 day of implantation, a ≈4-μm-thick layer of optically clear calcium carbonate is deposited on the transparent organic sheet. Within 2 days after implantation, the green organic sheet is deposited in a 1−10-mm-wide band on the circumference of the cover slip. The green sheet grows to a thickness of 5−15 μm. In general, calcium carbonate structures on the transparent sheet grow more quickly (≈5 μm/day) than those on the green sheet (≈1.2 μm/day) and are the first calcium carbonate structures to be overgrown with nacre.

Toward the center of the flat pearl, spherulitic and then more transparent platelike $CaCO_3$ morphologies were observed. This initial spherulitic deposition, which appears similar to the spherulitic morphology within the growth lines of the abalone shell, is followed by the formation of a nacre-like structure. The spherulitic $CaCO_3$ formed in this initial deposition on the flat pearls was at first suggested to be calcite,[1] but studies of the structure of the growth lines in native abalone shell by cathodoluminescence and Raman spectroscopy revealed the presence of aragonite rather than calcite within the growth lines,[8] prompting a re-evaluation of the initial deposition in the flat pearl.

In this paper, the crystal polymorphs, the interfaces between the growth lines and nacre, and the orientation relationship between blocklike/nacreous and spherulitic/nacreous microstructures have been characterized in native abalone shell and in flat pearls by scanning electron microscopy (SEM), transmission electron microscopy (TEM), and X-ray diffraction (XRD) analysis. Our aim is to give a detailed description of the microstructure of growth lines in native abalone shell and to compare them with similar features in flat pearls. We further characterize the calcitic prismatic microarchitecture using high-resolution scanning and transmission electron microscopy. Finally, we correct the earlier suggestion[1] that the blocklike and spherulitic structures within the growth lines in natural shells and the spherulitic structure in flat pearls are calcite—they are all aragonite, not calcite.

(7) Fritz, M.; Belcher, A. M.; Radmacher, M.; Walters, D. A.; Hansma, P. K.; Stucky, G. D.; Morse, D. E.; Mann, S. *Nature* **1994**, *371*, 49.

(8) Hawkes, G. P.; Day, R. W.; Wallace, M. W.; Nugent, K. W.; Bettiol, A. A.; Jamieson, D. N.; Williams, M. C. *J. Shellfish Res.* **1996**, *15*, 659.

Experimental Details

Red abalone (*Haliotis rufescens*) shells were cut into ≈1 × ≈0.5 × ≈0.5 cm specimens by a diamond saw and cross sections were mechanically polished and partially demineralized with EDTA. Plan-view samples could be prepared by cleaving shells along the green organic matrix within the growth lines, thus revealing both the blocklike and spherulitic layers on either side of the green organic matrix. The green matrix, which adheres strongly to the spherulitic layer, was then removed with sodium hypochlorite. Both the cross-sectional and plan-view sections were observed in a Hitachi-S4500 FEG SEM operating at 2 kV.

To identify the crystal structure of the blocklike and spherulitic layers, the plan-view samples were analyzed by X-ray diffraction (XRD). Cross-sectional and plan-view TEM thin foils were prepared using conventional ion-thinning techniques and were studied in a Philips CM 20 TEM operating at 200 kV.

For comparison, flat pearls were also studied by XRD, SEM, and TEM. These were grown by mineralizing 18-mm-diameter glass cover slip substrates inserted between the mantle tissue and the growing edge of the shell in red abalones maintained at 11 or 14.6 °C. The substrates were removed after 14, 21, and 28 days; the flat pearls were usually (and easily) removed from the glass substrates after drying. Cross-sectional SEM samples were prepared by gluing two pieces of flat pearl together using an epoxy adhesive, polishing a flat surface using 1200 SiC paper and 3-μm diamond abrasive, and briefly etching with EDTA. Plan-view TEM samples were prepared by one-sided ion thinning using a single gun incident on the side opposite to the glass substrates. Cross-sectional TEM samples were prepared from the same type of sample used for SEM analysis, again employing standard ion-thinning techniques.

The prismatic structure was also studied by both SEM and TEM to compare it with the calcitic layer of the flat pearls. Plan-view SEM samples were obtained from the growing edge of the native shell. Cross-sectional SEM samples were prepared by polishing and were partially decalcified with EDTA. Cross-sectional and plan-view TEM thin foils were again prepared using conventional ion-thinning techniques.

Results

Growth Lines in Native Abalone Shell. Figure 1a is a cross-sectional SEM micrograph showing a typical growth line in the red abalone shell. The green organic matrix is labeled G in the micrograph and extends from upper right to lower left. The upper left and lower right portions of this micrograph show the nacreous regions (labeled N). The blocklike layer (labeled B) lies between the upper left nacreous microstructure and the green organic matrix, while the spherulitic layer (labeled S) separates the green organic matrix and the lower right nacreous microstructure. The width of the growth lines in the red abalone shells we studied is variable, ranging from 15 to 70 μm. The thickness of the green organic matrix is also variable, ranging from 4 to 24 μm. In some growth lines, for example, Figure 1b, the green organic matrix is absent and spherulitic layers are likewise absent. The nacreous/blocklike interfacial structure in regions absent green matrix is similar to such interfaces in regions containing green matrix.

The structure of the blocklike layer is quite similar to that of nacre in that it contains a lamellar structure,

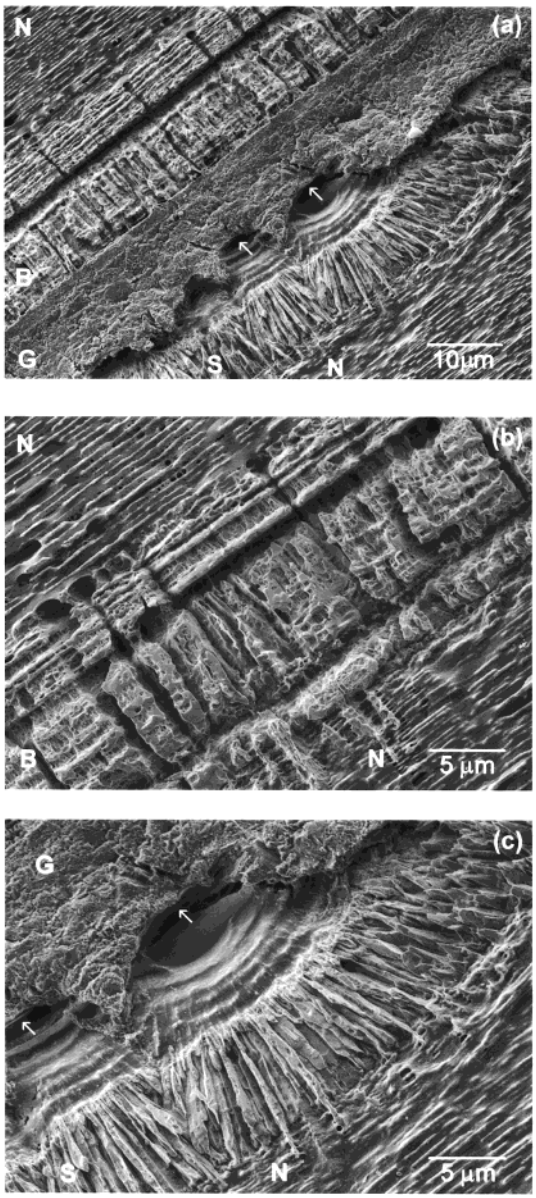

Figure 1. (a) Cross-sectional SEM micgrograph showing a typical growth line in native red abalone shell. (b) A growth line in the absence of green protein sheet and spherulitic layer. (c) The spherulitic structure at higher magnification. N, nacreous microstructure; B, blocklike microstructure; G, green organic matrix; S, spherulitic microstructure.

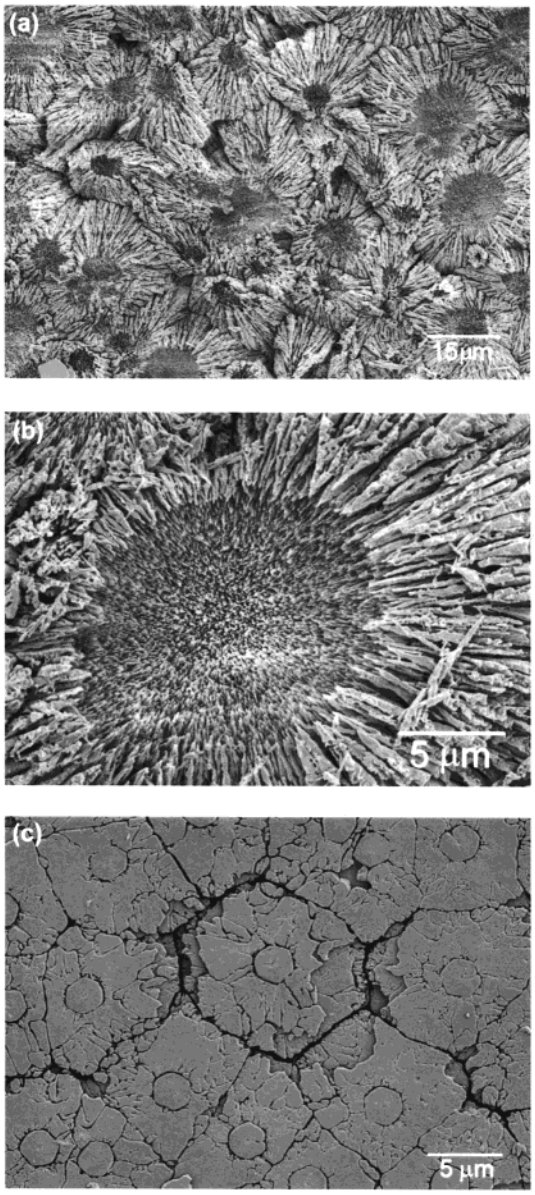

Figure 2. (a) Plan-view SEM micrograph of the spherulitic microstructure. (b) The spherulitic microstructure at higher magnification. (c) Plan-view SEM micrograph of the blocklike microstructure.

except that there is more vertically distributed structure in the blocklike than in the nacreous microstructure. The spherulitic layer (Figure 1a,c) consists of radially distributed elongated crystals which nucleate at a specific region (arrowed) of the green organic matrix; some of these elongated crystals then grow continuously into the adjacent nacreous structure. The long axes of the crystals in the center of the spherulites are more or less perpendicular to the adjacent individual nacreous tablets; those at the edge of the spherulites are more oblique than perpendicular to the adjacent tablets. The interface between the spherulitic and nacreous layers is not sharp. The thickness of the blocklike and spherulitic layers varies from 9 to 45 μm and from 8 to 16 μm, respectively.

Figure 2a is a plan-view SEM micrograph of the spherulitic microstructure; the resemblance to sunflowers is striking. The crystals at the center of the "sunflowers" are relatively fine-grained, with a diameter of $\approx$0.1 μm (Figure 2b). The crystals increase in size from the center to the outer edge and attain a maximum size of $\approx$2.5 μm in diameter. The diameters of the spherulites vary from 8 to 32 μm. The average distances between the center of two neighboring spherulites are $\approx$14 μm.

The units constituting the blocklike structure, again viewed parallel to the growth lines (Figure 2c), appear to be crystalline aggregates with four to six edges. Each individual aggregate contains a core surrounded by irregularly shaped crystals. The crystal aggregates in the shell studied vary from 5 to 11 μm in diameter; their sizes are similar to those of nacreous tablets.[1] The average distances between the centers of adjacent aggregates are $\approx$9 μm, somewhat smaller than those in the spherulitic layer. For comparison, the sizes of nacreous tablets vary from 5 to 10 μm and the average

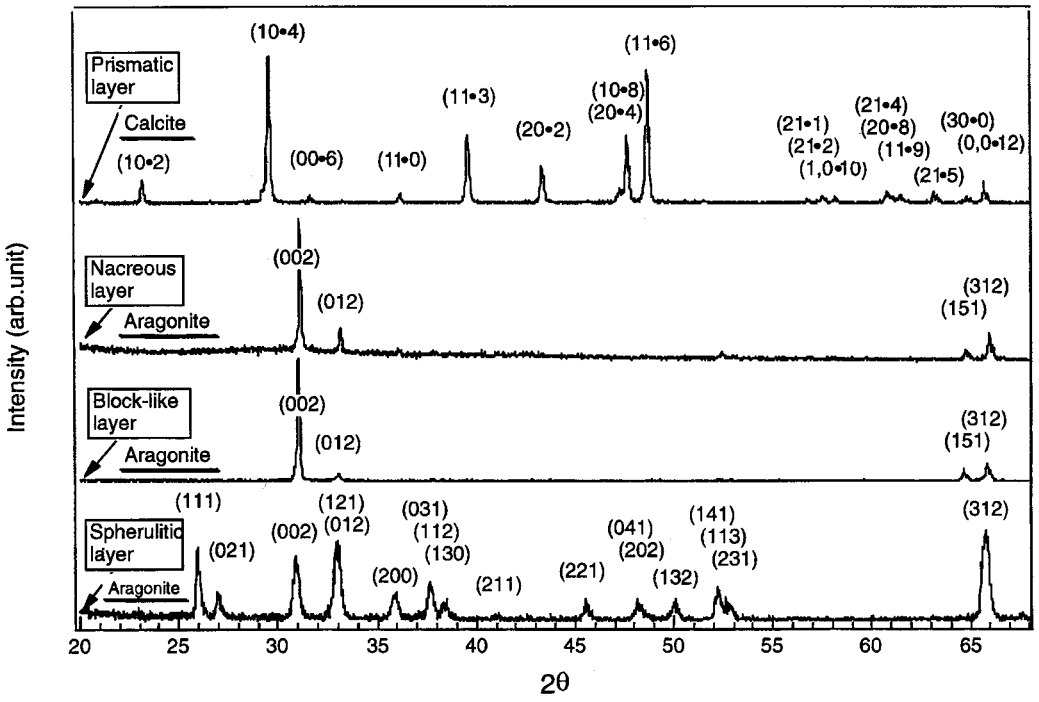

Figure 3. X-ray diffraction (XRD) pattern (Cu Kα radiation) of the nacreous, blocklike, and spherulitic structures. The XRD pattern from the calcitic prismatic layer is also shown as a control.

distances between two neighboring stacks of nacreous tablets are ≈9 μm, quite similar to individual crystals in the blocklike structure.

XRD was used to identify the crystal polymorph of the blocklike and spherulitic layers (Figure 3). For comparison, XRD patterns of the nacreous layer and prismatic calcitic layer are also shown in Figure 3. (The sample surfaces used for XRD analysis were parallel to the outer surface of the shell.) The crystals in both the blocklike and spherulitic layers are aragonite, the same as those in the nacreous regions of the shell. Both the nacreous and the blocklike microstructure are highly oriented, with an (002) preferred orientation. The preferential orientation of the crystals in the spherulitic layer is much less marked than either the blocklike or nacreous aragonite.

TEM studies have been made of plan-view samples of both the blocklike and spherulitic layers (see Figure 4a,b). The diffraction patterns in these figures were taken after the samples were tilted to a zone axis orientation. In Figure 4a, the protein interfaces (indicated by arrowheads) separating the core (labeled C) from the other irregularly shaped crystals in the blocklike microstructure can be clearly seen. The crystals are twinned on both (110) and (1$\bar{1}$0), the twin boundaries being indicated by the smaller arrows; twinning on these same systems have been reported in nacreous aragonite in red abalone shell.[9] Selected area diffraction patterns show that the individual aragonite aggregates in the blocklike structure are approximately single-crystal, with their orthorhombic **c** axes perpendicular to the top faces. On the basis of these SEM and TEM results, the blocklike structure can be defined as highly oriented aggregates of twinned aragonite crystals.

(9) Sarikaya, M.; Aksay, I. A. *Structure, Cellular Synthesis and Assembly of Biopolymers*; Case, T., Ed; Springer-Verlag: Berlin, 1992; pp 10−26.

In the plan-view micrograph of the elongated crystals within the spherulites, Figure 4b, only a thin slice of the crystals can be seen. There are many thin twin bands (in effect, many microtwins) within the crystals. This twinning also occurs on the (110) and (1$\bar{1}$0) systems. In some areas, there is a series of twin lamellae (labeled by arrowheads) on both (110) and (1$\bar{1}$0) planes. The extensive twinning is probably evidence for rapid mineralization of the spherulitic layer.

Parts a and b of Figure 5 are cross-sectional TEM micrographs showing the microstructure at the blocklike/nacreous interface. Figure 5a was obtained in strong Bragg contrast to show the continuity in crystallographic orientation of the crystals on either sides of the interface (labeled with arrowheads), which is nearly vertical in this micrograph, while Figure 5b was taken under weak beam-imaging conditions. There is an abrupt microstructural transition at the nacreous/blocklike interface; the terminating organic layers of the last nacreous tablet appear to serve as the substrate on which the blocklike structure forms. It is especially significant that the crystal aggregates in the blocklike layer maintain the orientation of the adjacent stacks of tablets in the nacreous structure; the crystalline material on either side of the nacreous/blocklike interface belong to a single aragonite crystal.

Parts c and d of Figure 5 are cross-sectional TEM micrographs from the spherulitic/nacreous interface. In Figure 5c, the elongated crystal marked "A" was tilted into a Bragg diffracting condition to show the continuity in orientation between the elongated crystal and the adjacent nacre; thus, the interface between the spherulitic and nacreous microstructures is very irregular. In all cases studied, the elongated crystals in the spherulitic layer maintained their orientation when they entered the nacreous layer.

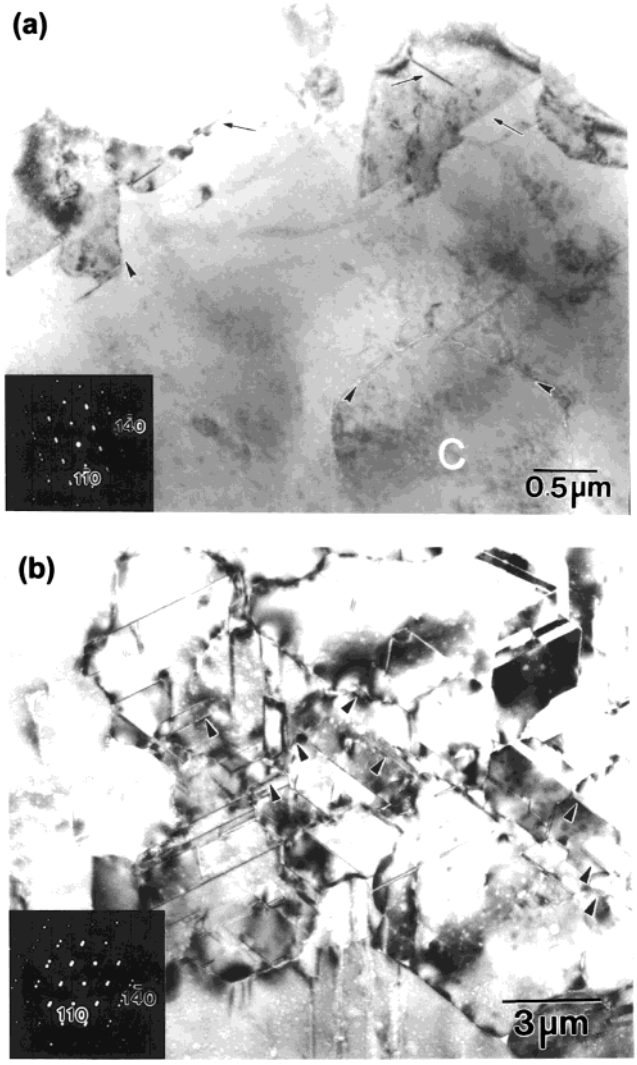

Figure 4. (a) Plan-view TEM micrograph and SAD pattern (zone axis orientation) of the blocklike structure. The twin boundaries are indicated by arrows, while grain boundaries are indicated by arrowheads. (b) Plan-view TEM micrograph and SAD pattern of the spherulitic structure. The twin lamellae are indicated by arrowheads.

Figure 5d is obtained at higher magnification from the upper right area of Figure 5c under weakly diffracting conditions. The crystals again show extensive twinning, the twin boundaries being marked by arrows. A grain boundary can also be seen in Figure 5d (the arrowheads).

Selected area diffraction patterns taken from cross sections of the nacreous tablets show that within an individual stack (Figure 6a), the tablets have approximately the same orientation, the maximum misorientation being ≈1.2°. Within an individual stack, the adjacent tablets are bridged by a mineral (indicated by arrows in Figure 6a,b), which amply demonstrates support for the new model for formation of the nacreous microarchitecture advanced earlier by our group.[10] In the face-on view, the adjacent tablets rotate by 0−45° around the [001] axis; that is, they can be said to have a turbostratic microstructure.

Flat Pearl. There are two distinguishable regions in flat pearls when viewed from the side adjacent to the glass substrates, those with a green and those with a white color (the white region actually has a light yellowish color). The white regions in the flat pearls grown at 14.6 °C cover from ca. one-eighth to ca. one-half of the 18-mm-diameter substrates, whereas the white portions of the flat pearls grown at 11 °C cover ca. one-half to ca. seven-eighths of the substrates. The green regions completely surround the white regions.

To study the structural difference in these two regions, all the flat pearls except those grown for 14 days were removed from their glass substrates and separated mechanically into white and green specimens. (The separation of the 14-day pearls was done with their substrates attached.) Parts a and b of Figure 7 are typical cross-sectional SEM micrographs from the white and green regions, respectively. The uppermost layers in these micrographs are epoxy layers (labeled E) used for specimen preparation (their location is where the glass substrates were situated during mineralization in the case of the 21- and 28-day flat pearls). In the white regions, the first layer grown on the glass substrate is calcite (labeled C), as will be demonstrated by the XRD and TEM data to be shown below. After calcite deposition ensues, green organic matrix (labeled G) is secreted directly onto the calcite layers. (In fact, because of the deposition of green organic matrix on top of the calcitic layer, the color of the white region is not pure white but has a light yellowish color (as shown in Figure 15a). The secretion of green organic matrix is followed by the growth of a spherulitic layer (labeled S) and then by nacre (labeled N). In the region between two neighboring spherulites, nacre forms directly on the green protein sheet.

The microstructure in the green regions of the flat pearl is the same as that in the white regions except that there is no calcite layer. In the green region (Figure 7b), the first layer grown on the substrates is the green organic matrix (labeled G), which is followed by a spherulitic layer and then by nacre. The morphology of the flat pearl above the green sheets in both regions is similar to that in the native abalone shell, except that there is no blocklike structure in flat pearls.

In a 14-day flat pearl, only the calcite layer was observed in the white region and only the green protein sheet in the green region (Figure 7c,d). In a 21-day flat pearl, a four-layered structure (Figure 7e)—calcite, green protein sheet, spherulitic layer and nacreous layer—was present in the white region and a two-layered structure (Figure 7f)—green protein sheet and spherulitic layer—in the green region. In a 28-day flat pearl, the four-layered structure in the white region (Figure 7a) is the same as that in a 21-day flat pearl, but a three-layered structure—green protein sheet, spherulitic layer, and nacreous layer—is formed in the green region (Figure 7b).

Figure 8 shows typical XRD patterns of the minerals adjacent to the glass substrates in the white region and the green region. The XRD pattern in the white regions is dominated by the calcite (10•4) phase (the intensity ratio of the calcite (10•4) peak to the aragonite (111)

(10) Schäffer, T. E.; Ionescu-Zanetti, C.; Proksch, R.; Fritz, M.; Walters, D. A.; Almqvist, N.; Zaremba, C. M.; Belcher, A. M.; Smith, B. L.; Stucky, G. D.; Morse, D. E.; Hansma, P. K. *Chem. Mater.* **1997**, *9*, 1731.

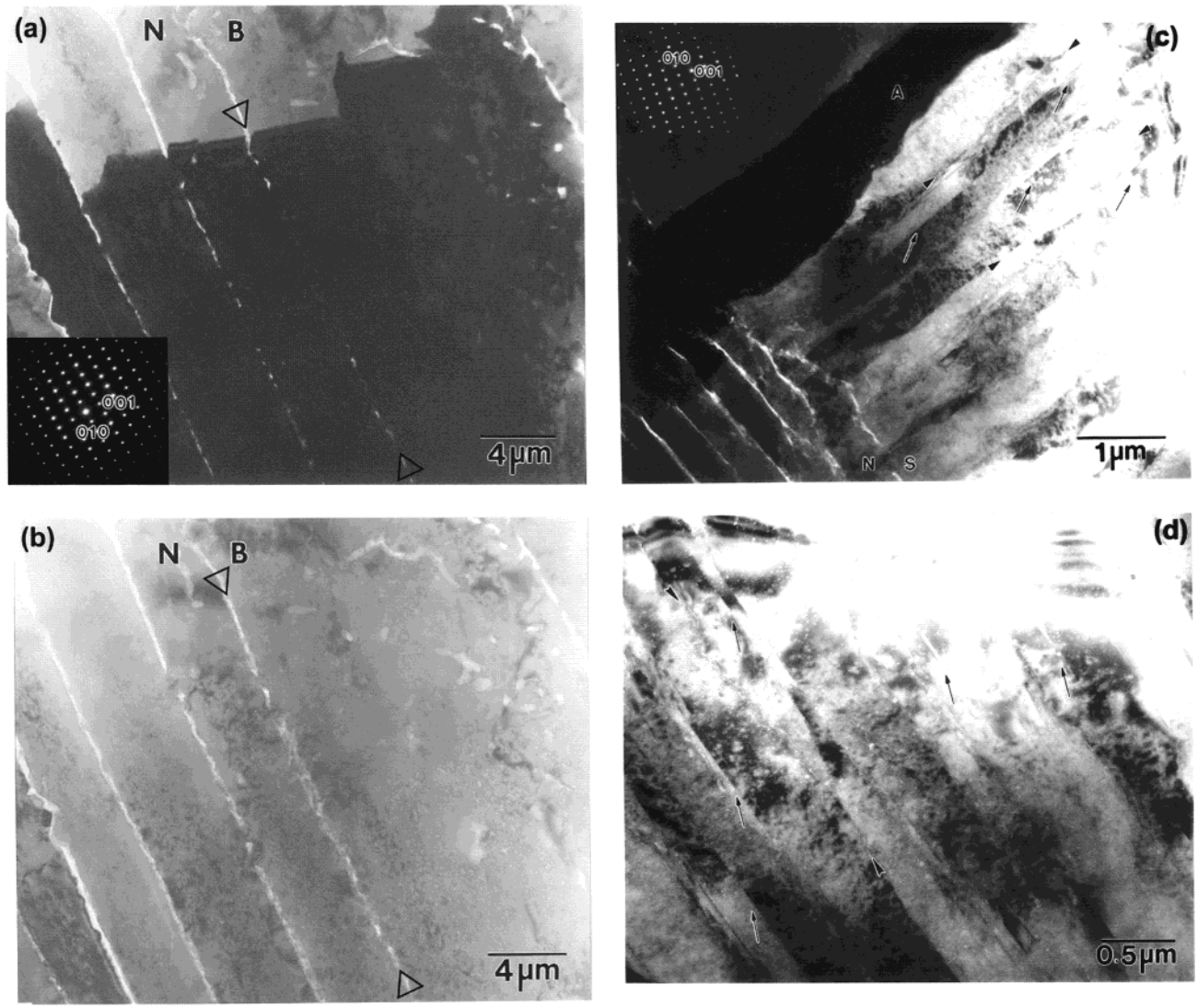

Figure 5. (a) Cross-sectional TEM micrograph of the blocklike microstructure in strong Bragg contrast. The inset is a zone axis SAD pattern of the blocklike microstructure. Arrowheads indicate the interface between blocklike and nacreous structure. (b) Cross-sectional TEM micrograph of the blocklike microstructure taken under a two-beam condition. Arrowheads indicate the interface between blocklike and nacreous structure. (c) Cross-sectional TEM micrograph of the spherulitic microstructure. Crystal "A" was tilted into a Bragg diffracting condition. The inset is a zone axis SAD pattern of crystal "A". (d) Cross-sectional TEM micrograph of the spherulitic microstructure at higher magnification. The arrowheads in (c) and (d) indicate the grain boundaries, while arrows indicate the twin boundaries. N, nacreous structure; B, blocklike structure; S, spherulitic structure.

peak is about 30), while in the green region, only aragonite peaks are present. The calcite is highly oriented, as only two calcite peaks are present in the 2θ range of 20−68° (for Cu Kα radiation), whereas the aragonite shows no obvious texture and is thus similar to the spherulitic microstructure in native abalone shell.

The microstructure of the first mineral grown on the glass substrates from the white (calcitic) regions of the flat pearl is highly inhomogeneous. Figure 9 shows four common morphologies. The most common ones, which are distributed throughout the entire area of the white region, are shown in parts b and c of Figure 9 and occupy approximately 30 and 40%, respectively, of this layer.

Figure 10a shows a bright field TEM micrograph, while several selected area diffraction (SAD) patterns from a white region obtained by large-angle tilting experiments are shown in Figure 10b−e; the SAD patterns fully confirm the XRD identification of calcite as the first mineral to form in the white region. Near the horizontal plane of the substrate, the calcite zone axes are $\langle\bar{3}2\bullet1\rangle$ and $\langle\bar{4}4\bullet1\rangle$ (Figure 10b,c), but calcite identification was further confirmed by tilting to the $\langle10\bullet4\rangle$ and $\langle11\bullet3\rangle$ zones (Figure 10d,e). Note that there are many organic materials, presumably protein occlusions within this first-formed mineral (Figure 10a) (the bright regions in this micrograph). Organic interfaces (indicated by arrowheads) are far from flat. No twin boundaries or dislocations were observed.

In the green region of the flat pearl, the crystals that form initially resemble those in the spherulitic layer in the native shell. Parts a and b of Figure 11 are SEM micrographs of the spherulitic crystals from a 21-day flat pearl; it is clear that the spherulites are clusters of elongated crystals. Although the spherulites barely cover the whole green sheet at this stage of flat-pearl growth, small tablets have already started to grow on top of the spherulites, as can be seen in the higher magnification SEM image, Figure 11b. At a later stage

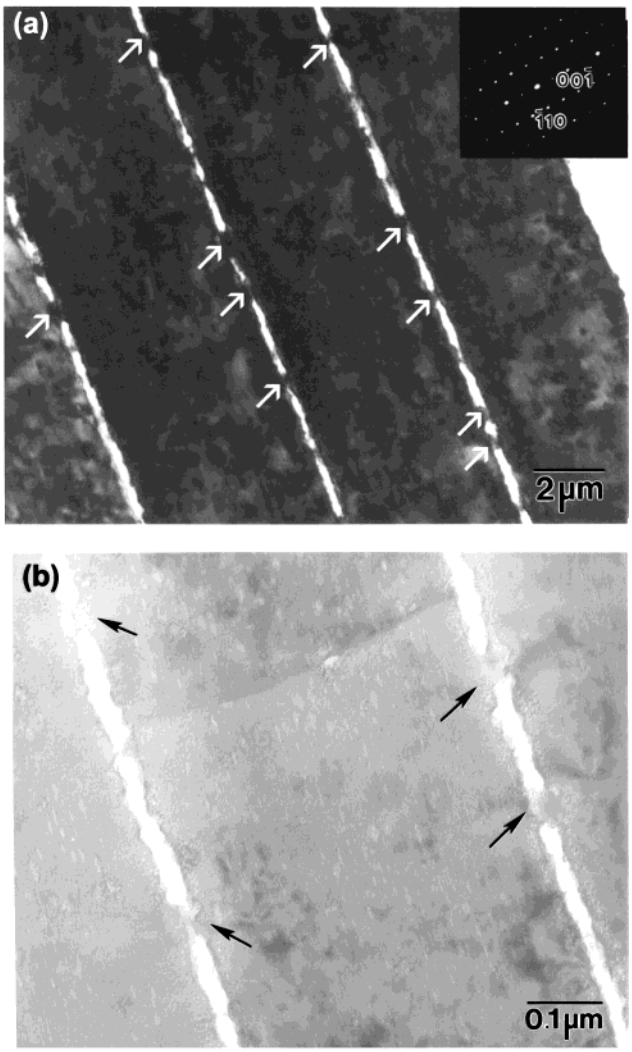

Figure 6. Cross-sectional TEM micrographs of the nacreous structure. (a) shows nacreous tablets in strong Bragg contrast, while the inset shows a zone axis SAD pattern; (b) shows a TEM micrograph in a two beam condition ($\bar{g}$ = 006). The arrows point to where tablets bridge.

of growth (Figure 12), the spherulites are overgrown by small nacreous tablets.

Figure 13 shows a bright field image in a plan-view TEM specimen (Figure 13a) and two SAD patterns of the elongated crystals grown on the secreted green sheet; the diffraction patterns correspond to the ⟨111⟩ and ⟨211⟩ zones of aragonite. These diffraction data again confirm the XRD data that the elongated crystals within the spherulites are aragonite, the same polymorph as is present within the spherulitic layer in native shell.

TEM has also been used to study the microstructure of the spherulitic layers above the green sheet in the white regions, cross-sectional foils being used for this purpose. Figure 14 shows a bright field image (Figure 14a) and SAD patterns (Figure 14b,c) from the spherulitic layer. The mineral in the spherulitic layer is aragonite, identical to that in the spherulites in the green regions. Thus, once green sheets are secreted, the polymorph that develops on the green matrix is aragonite and the overall microstructure is identical to that that develops in natural shell. Figure 15a is an optical photograph of a flat pearl and Figure 15b a very

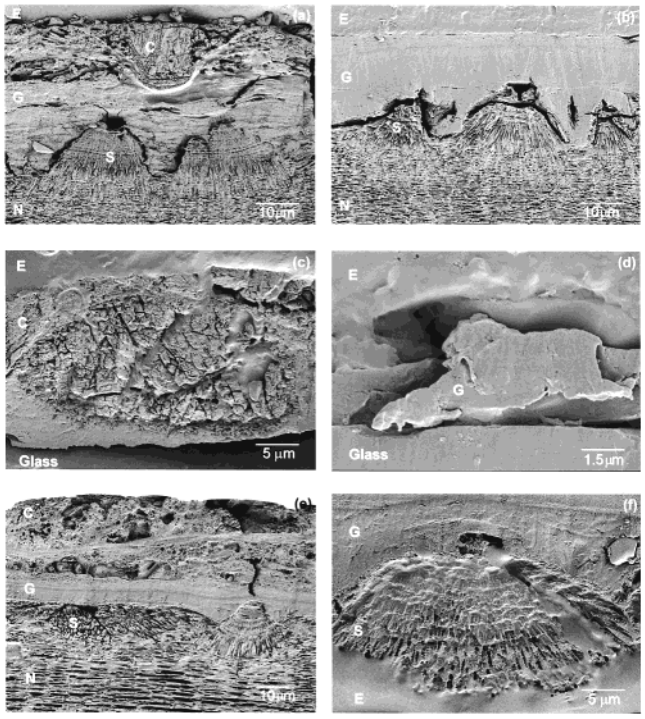

Figure 7. Cross-sectional SEM micrographs from the white region and the green region of the flat pearl. (a) and (b) are from the white and the green region of a 28-day pearl; (c) and (d) are from the white and the green region of a 14-day pearl; (e) and (f) are from the white and the green region of a 21-day pearl. E, epoxy layer; B, blocklike layer; G, green sheet; S, spherulitic layer; N, nacreous layer. The glass substrate has not been removed from (d).

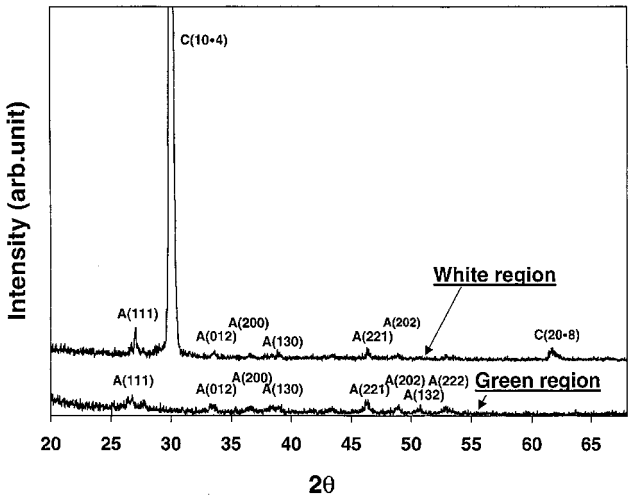

Figure 8. Typical X-ray spectra of the minerals initially deposited in the white region and green region (Cu Kα radiation).

simplified diagram of the structure of a flat pearl, summarizing the data contained in Figures 7−14.

Comparison of the Calcitic Layer in Flat Pearls and the Prismatic Layer in Native Shells. To compare the microstructure of the calcitic layer in flat pearls with the calcitic region that occurs in native shells, the prismatic layer at the growing edge of abalone shell was studied with SEM. Parts a and b of Figure 16 are plan-view SEM micrographs of the prismatic layer at two different magnifications. This layer consists of aggregates of prisms, the orientation

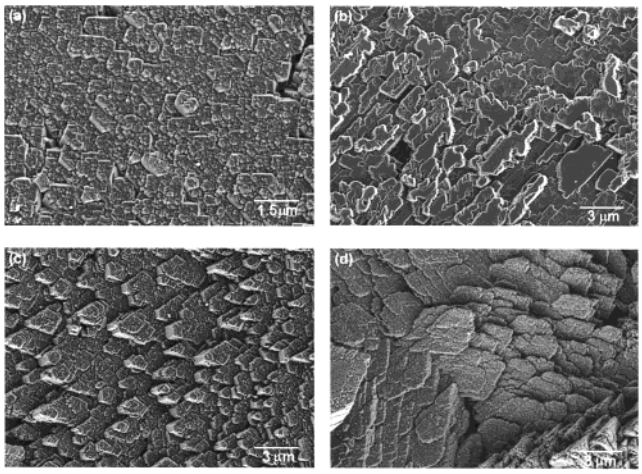

Figure 9. SEM micrographs of the first minerals grown in the white region of the flat pearl.

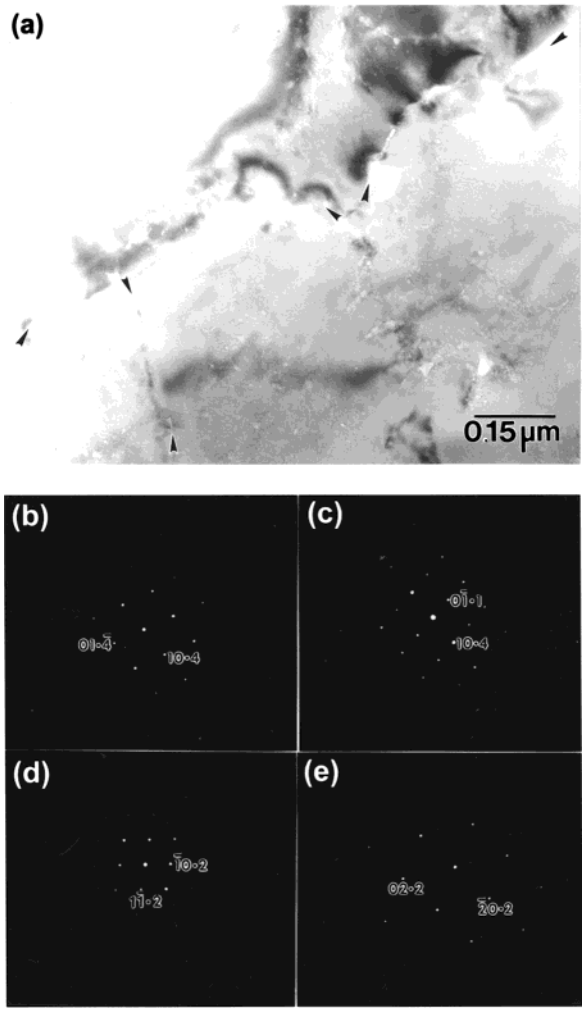

Figure 10. TEM micrograph (a) and zone axis SAD patterns ((b)−(e)) of the first minerals grown in the white region of the flat pearl. Arrowheads indicate the grain boundaries.

of the prisms being oblique to the growing inner surface of the shell. Within one aggregate (Figure 16b), all the prisms have the same orientation; the prism orientations vary considerably from one aggregate to another. This variation in orientation explains the modest texture in the X-ray pattern of the prismatic layer in native shell (Figure 3). In comparison, although the calcitic layers of flat pearls show more morphological variations

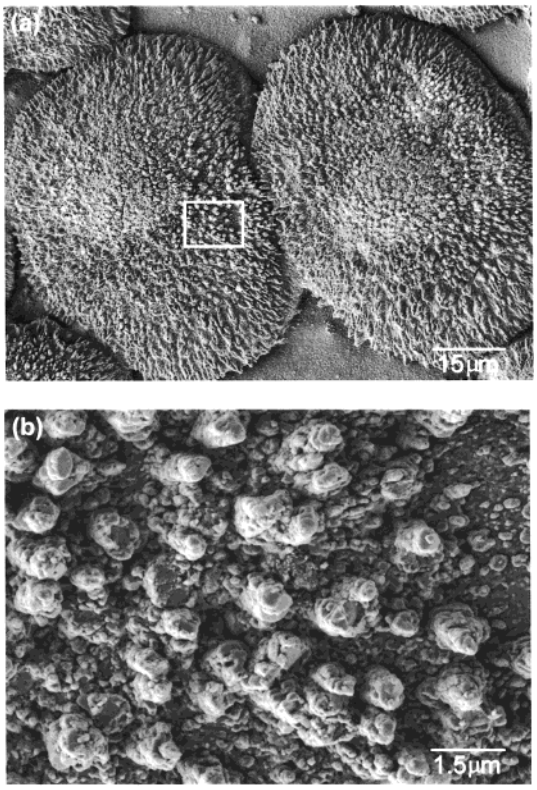

Figure 11. (a) SEM micrograph of the spherulitic microstructure from the green region of a flat pearl; (b) higher magnification image of the boxed area in (a).

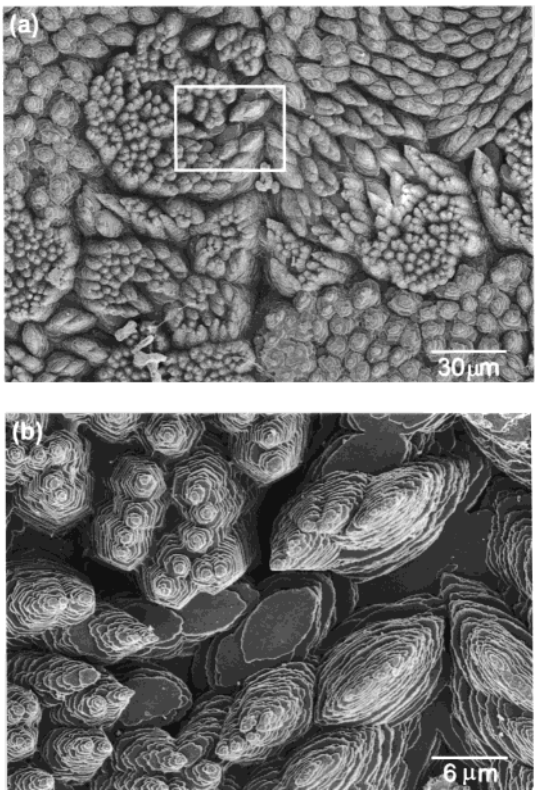

Figure 12. (a) SEM micrograph of the tablets grown on the spherulitic layer; (b) higher magnification image of the boxed area in (a).

(Figure 9), the orientation of the calcitic prisms is more or less perpendicular to the growing surface. The edges of the crystals of the calcite in flat pearls are not as flat as those in the prismatic layer in native shell.

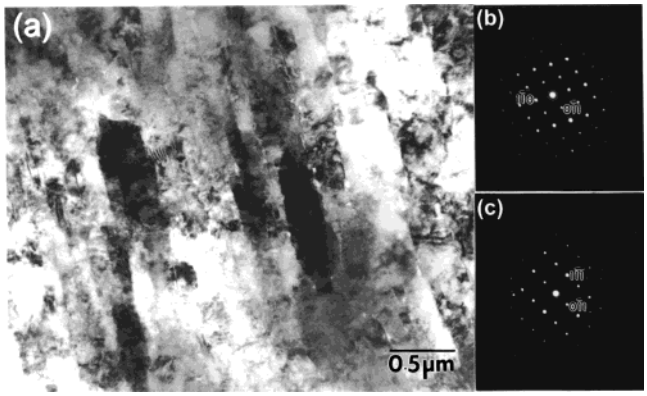

Figure 13. Plan-view TEM micrograph (a) and zone axis SAD patterns ((b) and (c)) of the spherulitic layer from the green region of the flat pearl.

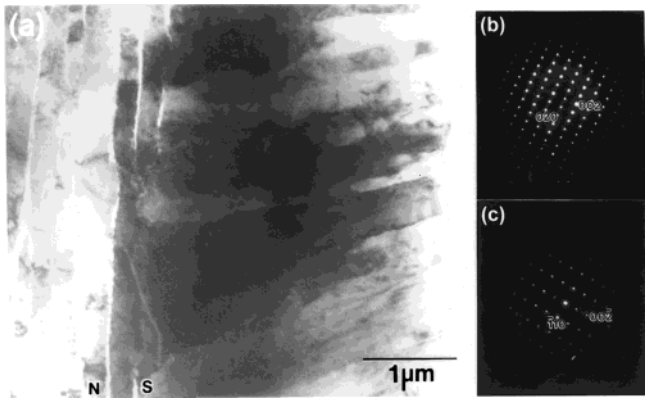

Figure 14. Cross-sectional TEM micrograph (a) and zone axis SAD patterns ((b) and (c)) of the spherulitic layer in the white region.

(a)

White region

Calcitic layer	Green region
Green sheet	Green sheet
Spherulitic layer	Spherulitic layer
Nacreous layer	Nacreous layer

(b)

Figure 15. (a) Optical photograph of a flat pearl and (b) schematic drawing showing the various components of flat pearls.

Green sheet and a spherulitic structure lie between the calcitic layer and the nacreous layer in flat pearls. However, neither green sheet nor a spherulitic structure is observed between the prismatic layer and the nacre in native shells. Figure 16c is a cross-sectional SEM micrograph of a partially decalcified sample. There is a clear interface between the prismatic and nacreous regions, the transition from prismatic to nacreous microstructure being abrupt.

Within the prismatic layer, there are fine bands oriented oblique to the prisms. Such bands are also observed in the calcitic layer in flat pearls (Figure 7a,c). Such bands were also observed by other investigators

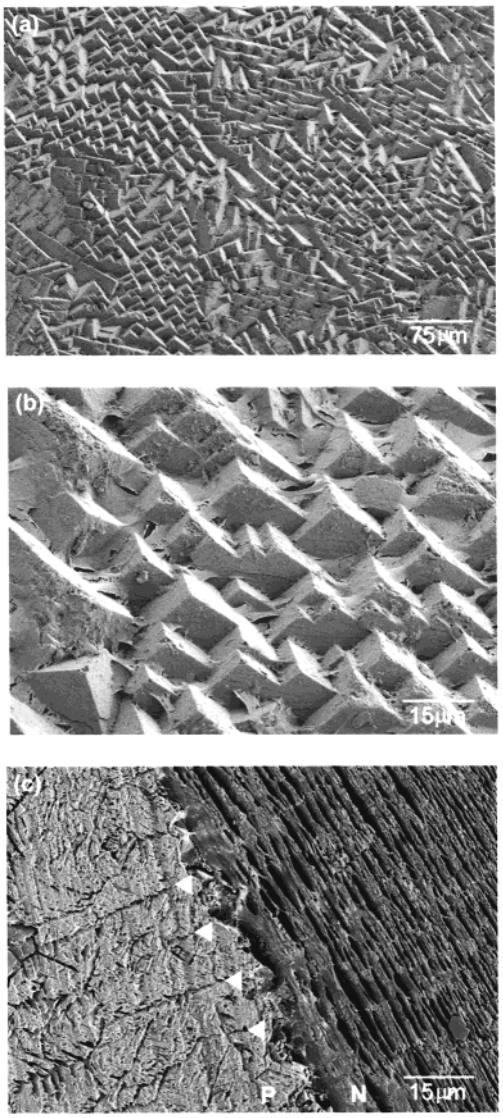

Figure 16. (a) Plan-view SEM micrograph of the prismatic layer at the growing edge of a red abalone shell. (b) Higher magnification image of (a). (c) Cross-sectional SEM micrograph showing the prismatic/nacreous structure interface. P, prismatic structure; N, nacreous structure; arrowheads, the prism interfaces.

in the prismatic layer of red abalone shell treated with the proteolytic enzyme trypsin.[3] The bands originate in the organic sheet which covers the growth surface of the prisms and then become embedded into the prisms when the shell continues to grow in a vertical direction.

As in the calcitic layer in flat pearls, there are no twin boundaries or dislocations in the prismatic layer of native shell (see Figure 17a), and the grain boundaries are quite planar. There are also organic materials (presumably protein occlusions), but not as many as in the calcitic layer of flat pearls.

Cross-sectional TEM micrograph shows a rough and wide interface (≈0.2-μm thick) separating the prismatic and nacreous structures (Figure 17d). The crystals in the nacreous region have a relatively irregular morphology at the interface, compared with those away from the interface. SAD patterns from the area above the interface (Figure 17e,f) indicate that the $CaCO_3$ is calcitic, while SAD patterns from the area below the interface (Figure 17g,h) indicate that the $CaCO_3$ is

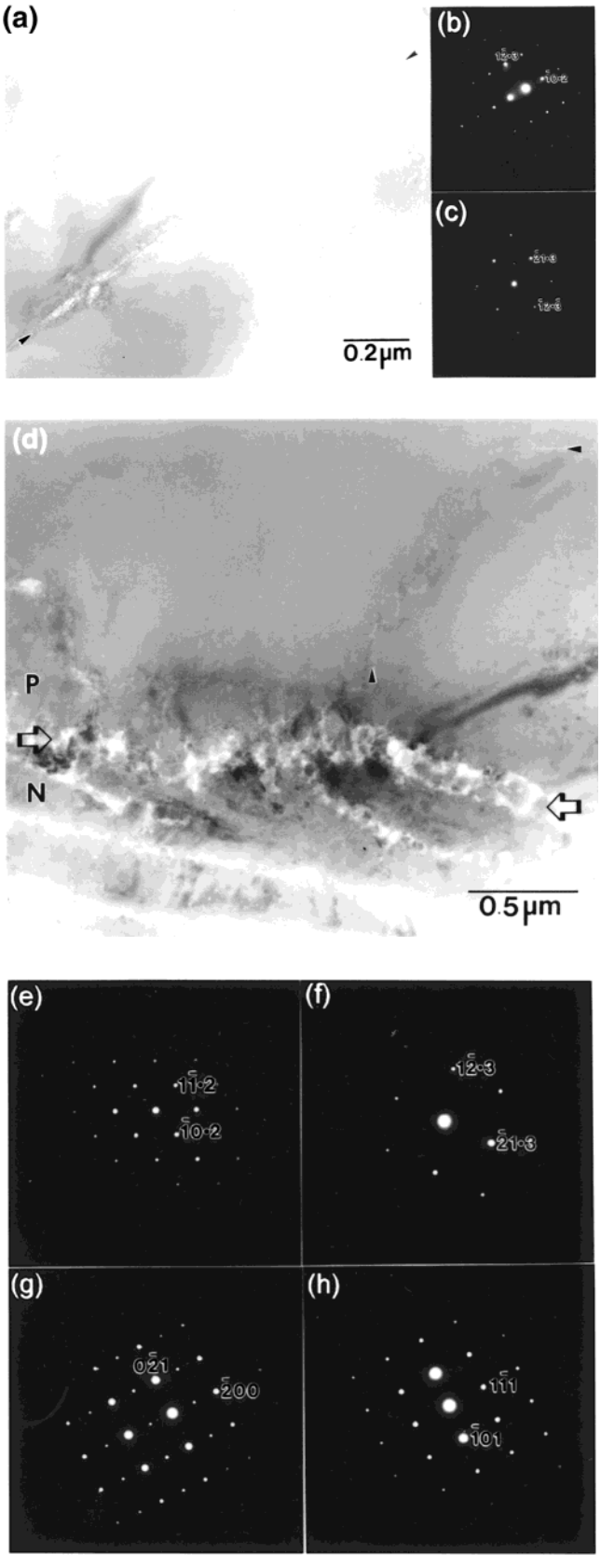

Figure 17. Plan-view TEM micrograph (a) and zone axis SAD patterns ((b) and (c)) of the prismatic layer. Arrowheads denote a grain boundary. (d) Cross-sectional TEM micrograph of the prismatic/nacreous structure interface. P, prismatic microstructure; N, nacreous microstructure; hollow arrows, prismatic/nacreous interface structure. (e) and (f) are zone-axis SAD patterns of the prismatic layer. (g) and (h) are zone-axis SAD patterns of the nacreous structure. P, prismatic microstructure; N, nacreous microstructure.

aragonite. Thus, the crystal structure switches abruptly from one polymorph to the other at the prismatic/nacreous interface in native shells.

Discussion

It is clear from our data that the minerals in both the blocklike and spherulitic microstructures in the growth lines of native red abalone shell are aragonite, the same mineral as that in the nacreous structure. The individual crystallites in the blocklike and spherulitic structures also have the same orientation as the neighboring minerals in the nacreous structure. The only matrix observed at the blocklike/nacreous and spherulitic/nacreous interfaces is that associated with the final layer of nacreous tablets.

Though the growth lines in the shells of various abalone species have been used to estimate the ages of abalone,[4−6] detailed studies of the structure of the growth lines are scarce. While cathodoluminescence and Raman spectroscopy suggested the presence of aragonite in these structures,[8] we know of no previous X-ray studies of the crystal structure of the growth lines in native abalone shell. In our earlier work,[1] it was assumed that the growth lines in natural shells contained calcite, but that assumption was based on preliminary XRD studies of flat pearls.

The flat pearls are grown by inserting abiotic substrates between the growing edge of the shell and the mantle of live red abalone. The initial minerals deposited on the outside edge of the insert and within the growth lines in such experiments are indeed calcite and thus differ significantly from the growth lines in native red abalone shell, which contain no calcite. The organism apparently responds to the insertion of foreign materials by calcite deposition, forming a layer that is in some sense similar to the external layer in native shells; this is followed by deposition of green organic matrix that participates in the induction of spherulitic aragonite and then nacreous aragonite; in this regard, the flat pearls are nearly exact mimics of the growth lines in native shells.

The composition of the organic matrix of shells produced on a plastic substrate inserted between the mantle and the shell have been compared[11] with that of normal aragonitic shell of the mollusc *Pomacea paludosa*. A lower glycine content and higher amino acid compositions were found in the early stages of such induced biomineralization, and a correspondingly higher percentage of calcite was formed. When the amino acid composition of the shell formed on the plastic substrate approached that of normal shell, aragonitic $CaCO_3$ with only a trace of calcite was obtained. A change of polymorph has also been found on abiotic substrates inserted in *Elliptio*, which normally has an aragonitic shell.[12] In this case, all three polymorphs of $CaCO_3$ (calcite, aragonite, and vaterite) were deposited when glass was inserted adjacent to the animal's mantle. A very striking change is observed in the organization of the organic matrix and the orientation of the subsequent $CaCO_3$ phase when single-crystal MoS_2 is inserted as a

(11) Meenakshi, V. R.; Blackwelder, P. L.; Hare, P. E.; Wilbur, K. M.; Watabe, N. *Comp. Biochem. Physiol.* **1975**, *50A*, 347.
(12) Wilbur, K. M.; Watabe, N. *N. Ann. N. Y. Acad. Sci.* **1963**, *109*, 82.

substrate,[1] further illustrating how dramatically the surface chemistry of the inorganic substrate can modify the biomineralization.

It is significant that, after the insertion of the foreign materials, alteration of the organic matrix involves changes in the amino acid composition. The organic matrix in mollusc shells has a profound influence on both the polymorph of $CaCO_3$ formed and its morphology. Recently, we have convincingly demonstrated the role of shell proteins in the control of crystal polymorph during in vitro crystal growth, presumably due to the interaction of the soluble proteins with specific crystal planes of the $CaCO_3$ polymorphs.[13] The experimental systems consisted of both insoluble organic matrix and soluble, mineral-specific proteins extracted from either aragonitic or calcitic portions of the abalone shell, which were added to aqueous solutions in which $CaCO_3$ was crystallizing. The mineral-specific soluble proteins controlled the polymorph formed in such *in vitro* crystallization experiments with high fidelity.

The role of the insoluble proteins is unclear. It has been suggested[14,15] that the insoluble matrix is important in providing a microenvironment favorable for the formation of certain polymorphs. In the growth lines of native red abalone shell, a green insoluble organic matrix is secreted on the blocklike layer, whose nature is quite different from the matrix surrounding tablets in the nacreous structure. Yet the crystals nucleated on the green matrix in the spherulitic layers still retain the nacreous polymorph and orientation. The likeliest explanation is that simple homoepitaxy is at play in the regions shown in Figure 5 (the blocklike/nacreous and spherulitic/nacreous interfaces), with the nacreous morphology being controlled by insoluble proteins.

This last point is important and deserving of further discussion. The polymorph type is continuous at the interfaces of the nacreous/blocklike structures, and the nacreous and the blocklike structure have the same orientation—both microstructures have a preferred (002) orientation perpendicular to the outer surface of the shell. The minerals at the nacreous/blocklike interfaces are bridged in the same way as are the tablets in the nacreous structure. Inasmuch as the minerals in both structures have similar morphology, and both structures have similar dimensions, we infer that the blocklike structure is an abnormal morphology of nacre produced prior to or coincident with the temporary cessation of the shell growth.

Some of the crystals within the spherulitic layers grow into the nacreous layer. In this situation, the minerals in the nacreous layer and the connected crystals in the spherulitic layer again have the same orientation, and insoluble matrix is again absent on the spherulitic layer prior to the change of microstructure.

Spherulitic structures also exist in other biomineralized tissue and in synthetic systems. Aragonitic spherulites have been observed in the otoliths of fish, in scleractinian corals, and in regenerated shells,[16−18] while calcitic spherulites are found in egg shells.[17] Spherulitic structures in devitrified silicate glasses[19] and in organic high polymers[20] are well-known. Spherulites are often formed in rapid crystallizing solutions and when there is limited nucleation of a crystalline phase in a very viscous medium. However, spherulitic layers are absent in the growth lines in native red abalone shell when the green organic matrix is absent. Thus, in this particular example, the formation of the spherulitic structure must be related to the nature of the green organic matrix. We believe that a protein which controls the kinetics of aragonite formation in the nacreous tabular microstructure is absent in the green matrix; this either causes rapid crystallization, as in inorganic glasses and high polymers, or causes spherulitic growth because of limited nucleation.

The deposition of growth lines corresponds with sea temperature maxima, minima, and spawning; it has been suggested to either result from or serve as a self-protection response to changes in environmental conditions.[4−6] The cessation of nacre deposition involves the deposition of a blocklike layer and the secretion of a green organic matrix. The green organic matrix is very stable and has good resistance to a wide range of denaturing agents, which can protect the shell from dissolution. When the environment is again favorable for growth, crystals nucleate on a few sites on the green organic matrix and grow rapidly to form a spherulitic structure.

Conclusions

Both blocklike and spherulitic structures in native red abalone shells are composed of aragonitic $CaCO_3$, the same polymorph as in the nacreous structure. The minerals in both structures have the same orientation as in the adjacent tablets in the nacre. The only matrix observed at the blocklike/nacreous and spherulitic/nacreous interfaces is associated with the final layer of nacreous tablets.

The microstructures within flat pearls, produced by inserting glass substrates between the mantle tissue and the shell of living animals, is similar in many regards to the growth lines. Calcite is initially formed as a white deposit on the center of the glass substrates, but the remaining area of the substrate and the calcite are soon covered by green matrix, which is similar in composition to the green matrix within the growth lines in natural abalone shell. (Calcite is absent in growth lines in natural shells.) Spherulitic aragonite then forms on the green matrix, which soon gives way to a nacreous aragonitic microstructure. For all intents and purposes, the microstructures adjacent to the green matrix in flat pearls and adjacent to the green matrix within the growth lines in natural shells are identical.

The blocklike microstructure that precedes secretion of the green matrix in growth lines in natural shell is

(13) Belcher, A. M.; Wu, X. H.; Christensen, R. J.; Hansma, P. K.; Stucky, G. D.; Morse, D. E. *Nature* **1996**, *381*, 56.
(14) Falini, G.; Albeck, S.; Weiner, S.; Addadi, L. *Science* **1996**, *271*, 67.
(15) Levi, Y.; Albeck, S.; Brack, A.; Weiner, S.; Addadi, L. *Chem. Eur. J.* **1998**, *4*, 389.
(16) Addadi, L.; Weiner, S. *Angew. Chem. Int. Ed. Engl.* **1992**, *31*, 153.
(17) Lowenstam, H. A.; Weiner, S. *On Biomineralization*; Oxford University Press: New York, 1989.
(18) Watabe, N. *J. Cryst. Growth* **1974**, *24/25*. 116.
(19) Johannsen, A, *A descriptive petrograph of igneous rocks*; University of Chicago Press: Chicago, IL, 1931; Vol. 1; pp 15−19.
(20) Keith, H. D. *The Physics and Chemistry of the Organic Solid State*; Fox, D., Labes, M. M., Weissberger, A., Eds.; Interscience Publishers: New York, 1963; Vol. 1, pp 462−542.

absent in the flat pearl. It apparently records the temporary cessation of shell formation; subsequent mineralization resumes in the following sequence: green matrix, spherulitic aragonite, and nacreous aragonite.

Acknowledgment. We would like to thank Martina Michenfelder for growing the flat pearl samples. The work at CWRU was supported by EPRI and that at UCSB by the National Science Foundation (Grant DMR-9634396), the Office of Naval Research, and the U.S. Army Research Office Multidisciplinary University Research Initiative Program.

CM011739Q